Conductance and addition spectrum of a 2×2 quantum-dot array in the extended Hubbard model

Zhiming Yu, Thomas Heinzel,* and A. T. Johnson
Department of Physics and Astronomy, David Rittenhouse Laboratory, 209 S. 33rd Street, University of Pennsylvania, Philadelphia, Pennsylvania 19104
(Received 22 January 1997)

We have studied the conductance and addition spectrum of a 2×2 quantum-dot array in the extended Hubbard model, i.e., when the dots are coupled to each other by both interdot tunneling and an interdot Coulomb interaction. Under parameters appropriate for experiment, both the addition spectrum and the conductance show a dramatic *qualitative* difference between a situation dominated by interdot Coulomb interaction and the pure Hubbard model. We calculate how, in the general case, these different contributions influence the spectra. The effects of various types of disorder are discussed. [S0163-1829(97)07520-6]

Collections of coupled quantum dots might serve as a controllable experimental system for the largely unexplored physics of strongly correlated electrons.[1–7] Quantum dot arrays have been fabricated in the Ga[Al]As two-dimensional electron gas, defined by etching,[8] or surface gates.[9–14] Other realizations based on molecular nanostructures[15] or semiconductor nanoclusters[16] may emerge soon. Recent theoretical work has discussed potential applications of such arrays.[17]

An isolated quantum dot can be characterized by an on-site electron-electron interaction energy U and a set of discrete energy levels $\{\varepsilon_l\}$. When quantum dots are near enough to couple to one another, two new energy scales emerge. The first is an interdot charging energy W. Here we assume that U and W are described by a set of classical capacitances between the quantum dots and between each quantum dot and electrical ground. The second energy, describing the formation of a ''chemical bond'' between quantum dot ''artificial atoms,''[18,19] is related to the tunnel matrix element t between equivalent single-particle states on neighboring dots. Both interactions have a profound effect on the array's electron addition spectrum and conductance.

Theoretical work on the ''charging model,'' where U and W are the dominant energies and the discreteness of the dot energy levels is ignored, has been verified in arrays of metal islands coupled by tunnel junctions.[20] An intermediate regime, where the dot discrete energy level structure is significant, but tunneling between dots is incoherent, has been accessed in experiment.[11]

Experiments attempting to probe the ''Hubbard model'' regime ($U\gg t\gg W$), where self-charging and coherent tunneling are critical, have remained difficult to interpret.[21,22] Theory predicts that for linear arrays of quantum dots both the charging model and the Hubbard model lead to similar fine structure in the addition spectrum and conductance. In fact, for an array of two quantum dots in series, the predictions of the two theories are identical.[23] In order to distinguish between the two pictures, assumptions must be made about the relative strengths of interdot capacitances compared to interdot coupling constants,[9–14,24] both of which are difficult to measure directly. Furthermore, the interdot tunneling and the interdot capacitance cannot be tuned independently in experiments performed so far: changing the voltage applied to a gate that controls the tunneling between the dots influences the separation of the dots, and hence the capacitance they form, as well.

It would thus be very desirable to study a dot array geometry showing a *qualitative* difference between coherent tunneling and charging in the conductance or in the addition spectrum, experimentally accessible via transport and capacitance measurements, respectively. In the present paper, we show that a 2×2 quantum-dot array is such a system.

After introducing the model used to calculate the conductance and the addition spectrum as a function of the chemical potential, we consider two limiting cases, the pure Hubbard model and the classical Coulomb interaction model. In the regime of weak interdot tunneling, the Hubbard model produces a triplet structure in both the conductance and the addition spectrum, i.e., our results for the addition spectrum reduce to those of Ref. 3. The interdot Coulomb interaction, however, generates a characteristic doublet structure, implying that the two regimes can be distinguished in experiment. We proceed by studying the general case, for parameters adapted to state-of-the-art fabrication techniques and experimentally achievable temperatures. Finally we discuss the effects of different types of disorder, namely in the dot energy levels, the interdot tunneling rates, and the interdot and on-site Coulomb interactions.

A schematic view of the dot array is shown in the inset of Fig. 1(a). Four identical quantum dots are arranged in a square lattice. They couple to each other via nearest-neighbor interdot capacitances C and interdot tunneling matrix elements t. We ignore tunneling and capacitances between dots diagonally opposite to each other. Two of the dots also couple to nearby leads, and each dot has a capacitance C_g to a backgate, whose voltage tunes the chemical potential of the system. This geometry can be realized easily in experiments.[9,10,12] Calculations for other schemes of coupling to the leads are straightforward, and give qualitatively similar results. In the extended Hubbard model, the Hamiltonian reads

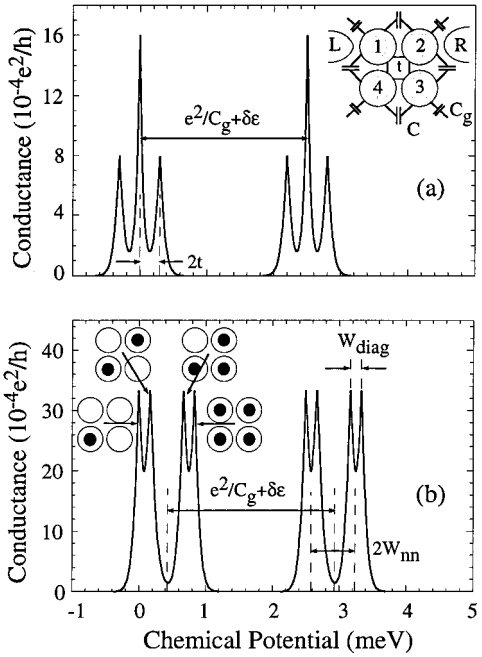

FIG. 1. (a) Conductance as a function of the chemical potential of the quantum dot array in the Hubbard model. The parameters are $k_BT=50\ \mu$eV, single dot charging energy $e^2/C_g=2$ meV, and energy level spacing in each dot $\Delta\varepsilon=0.5$ meV. (b) Conductance for the charging model consists of a pair of doublets. Temperature and energy level spacing are as in (a); we take $C/C_g=0.5$, so $U=1.17$ meV, $W_{nn}=0.33$ meV, and $W_{diag}=0.17$ meV. Inset: 2×2 array geometry.

$$\hat{H}=\sum_{i,\alpha}\varepsilon_{i\alpha}\hat{c}^{+}_{i\alpha}\hat{c}_{i\alpha}+\frac{1}{2}\sum_{i}U_i\hat{n}_i(\hat{n}_i-1)+\sum_{i<j}W_{ij}\hat{n}_i\hat{n}_j+\sum_{i<j,\alpha}t_{ij,\alpha}(\hat{c}^{+}_{i\alpha}\hat{c}_{j\alpha}+\hat{c}^{+}_{j\alpha}\hat{c}_{i\alpha}). \quad (1)$$

The first term describes the discrete energy levels of the individual quantum dots. The index i is the site, and α enumerates the energy levels. $\varepsilon_{i\alpha}$ is the energy of this particular state, and $\hat{c}^{+}_{i\alpha}$ and $\hat{c}_{i\alpha}$ are the creation and annihilation operators, respectively. Our calculations include two energy levels in each dot. The second term describes the on-site Coulomb interaction, where U_i is the Coulomb repulsion on the ith dot, and $\hat{n}_i=\Sigma_\alpha\hat{c}^{+}_{i\alpha}\hat{c}_{i\alpha}$ is the number operator. The third term gives the Coulomb interaction between electrons in dots i and j. W_{ij} is the Coulomb repulsion between dot i and dot j. By calculating the electrostatic energy of the dot array in a classical capacitance matrix approach, we obtain the U_i and the interdot charging energies, W_{nn} for nearest-neighbor dots and W_{diag} for dots diagonally opposite to each other.[25] The fourth term describes the electron tunneling between dots, where $t_{ij,\alpha}$ is the tunneling matrix element between the α states on dot i and dot j. We neglect tunneling between nonresonant states by only allowing tunneling between identical states in different dots, and we only allow tunneling between neighboring dots. Spin degeneracy is not included in Eq. (1). This degeneracy can be removed by a magnetic field, applied perpendicular to the plane of the array.

The eigenvalues and the eigenfunctions of the resulting 256×256 Hamiltonian matrix [Eq. (2)] are obtained by using Lanzco's technique.[26,27] We calculate both the addition spectrum and the conductance of the dot array. The addition spectrum $\partial\langle n\rangle/\partial\mu=k_BT\partial^2(\ln Z)/\partial\mu^2$ is calculated by determining the grand partition function $Z=\Sigma_{n,i}\exp[-(E_{n,i}-n\mu)/k_BT]$. Here, $E_{n,i}$ is the energy eigenvalue of the ith many-body state with n electrons in the array, and μ denotes the chemical potential. Since $\partial\langle n\rangle/\partial\mu=\partial Q/e^2\partial V$, the addition spectrum can be obtained experimentally by measuring the differential capacitance as a function of the voltage V applied to the backgate. This formula for the addition spectrum is appropriate for very weak coupling between the array and a particle reservoir (i.e., the backgate), which is the regime usually accessed in experiment.[28,29]

To calculate the conductance, we add the tunneling Hamiltonian $\sum_{\substack{k\in L,R\\ i\alpha}}V_{ki\alpha}(\hat{c}^{+}_{i\alpha}\hat{c}_{k\alpha}+\hat{c}^{+}_{k\alpha}\hat{c}_{i\alpha})+\Sigma_{k\alpha}\varepsilon_{k\alpha}\hat{c}^{+}_{k\alpha}\hat{c}_{k\alpha}$ to the Hamiltonian (1), and treat it in first-order perturbation theory. The first term describes the tunneling between state α in dot i and lead k [left (L) or right (R)], with tunneling matrix $V_{ki\alpha}$. We choose a coupling scheme of the dot array to leads as indicated in Fig. 1(a), i.e., we set $V_{L1\alpha}=V_{R2\alpha}=10\ \mu$eV; all other coefficients are set to zero. The second term gives the energy in the leads, where $\varepsilon_{k\alpha}$ is the energy of state α in lead k, and $\hat{c}^{+}_{k\alpha}$ ($\hat{c}_{k\alpha}$) is the creation (annihilation) operator for electrons in the leads. As discussed elsewhere,[30,31] we obtain for the conductance G of the dot array

$$G=\frac{e^2}{k_BT}\sum_{n=1}^{N_{max}}\sum_{ij}\frac{\Gamma^{L}_{nij}\Gamma^{R}_{nij}}{\Gamma^{L}_{nij}+\Gamma^{R}_{nij}}P^{eq}_{n,i}\times[1-f(E_{n,i}-E_{n-1,j}-\mu)]. \quad (2)$$

Here, N_{max} is the maximum possible number of electrons in the dot array. $\Gamma^{L,R}_{nij}$ is the transmission matrix from the ith n-particle state to the jth $(n-1)$-particle state via tunneling to the left or right reservior, given by $\Gamma^{L,R}_{nij}=2\pi\Sigma_\alpha|\langle n,i|V_{k1\alpha}\hat{c}^{+}_{1\alpha}|n-1,j\rangle|^2$. $P^{eq}_{n,i}$ is the equilibrium probability for occupying the eigenstate (n,i) with eigenvalue $E_{n,i}$, given by $P^{eq}_{n,i}=(1/Z)\exp[-(E_{n,i}-n\mu)/k_BT]$, and $f(E_{n,i}-E_{n-1,i}-\mu)$ is the Fermi-Dirac distribution function. Equation (2) applies when the coupling of the dot array to the leads is weak, i.e., $V_{k\alpha}\ll\delta\varepsilon,\ k_BT$. This calculated conductance can be measured in a two-terminal transport configuration.

Throughout the whole paper, we set $e^2/C_g=2$ meV. This corresponds to the charging energy of a single dot for $C=0$. The temperature is set to $T=550$ mK ($k_BT=50\ \mu$eV), easily realized in a ^{3}He/^{4}He dilution refrigerator. We choose an energy splitting between discrete levels $\delta\varepsilon_i=0.5$ meV. The interdot charging energy W_{ij} is determined by the interdot capacitance C, and $t_{ij,\alpha}$ by the wave-function overlap.

First, we consider, in the absence of disorder, two limiting cases, namely the Hubbard model and the situation dominated by the interdot Coulomb blockade (Fig. 1). For the Hubbard model, the addition spectrum has already been thoroughly studied by Stafford and das Sarma.[3] At low tunneling matrix elements, the authors find a triplet structure with a twofold degenerate center peak and two satellite peaks, sepa-

rated by $2t$ from the center peak. Basically, this structure corresponds to the onset of a discretized energy band. As t increases, these minibands spread out in energy and finally start to overlap. The separation of the two miniband centers is $e^2/C_g+\delta\varepsilon$. In the absence of disorder, the conductance shows exactly the same structure [Fig. 1(a)]. An interdot Coulomb interaction, on the other hand, produces a very different structure [Fig. 1(b)]. The conductance (as well as the addition spectrum, not shown here) shows characteristic doublets, with the peak splittings being determined by W_{ij}. As in the Hubbard limit, the separation of the minibands is determined by $e^2/C_g+\delta\varepsilon$.

We can understand this structure in terms of classical electrostatics. Consider adding four electrons to an empty array. When $C=0$, the dots are independent of each other. An electron is added to each dot at the same chemical potential, so the spectrum is a single fourfold degenerate peak. In contrast, when $C\ll C_g$ the degeneracy is lifted. The first electron will randomly occupy one of the four sites, and the second electron will occupy the site diagonally opposite to the first. It feels, however, the presence of the first electron, and hence the addition of the second electron requires W_{diag} more energy than the first. The third electron randomly occupies one of the two remaining empty sites. Two electrons are sitting in its neighbor dots, thus adding this electron requires the additional energy of $2W_{\mathrm{nn}}-W_{\mathrm{diag}}$. Similar to the second electron, the fourth electron feels the presence of the third electron, and an additional energy of W_{diag} is needed to add it to the last unoccupied site. Under increasing C, this modulation of the peak separation is reduced, leading to equidistant peaks inside one miniband for $C\gg C_g$, which corresponds to the formation of one large conducting region.

We proceed by studying the more general situation, the extended Hubbard model (Fig. 2). The evolution of the addition spectrum as a function of the ratio C/C_g, for constant t, is shown in Fig. 2(a). At $C=0$, the addition spectrum has the typical triplet structure of Fig. 1(a). As C increases, the degenerate states that make up the center peak split, and the energy splitting of the satellite peaks increases, as expected from the discussion of Fig. 1(b). The wide gap between the triplets is reduced, and as C/C_g becomes much larger than 1, the addition spectrum evolves in a set of nearly equally spaced, nondegenerate peaks. Their separation is given by the effective charging energy of one dot, plus contributions due to the energy level spacing and the interdot tunneling. For any value of C/C_g, the spectrum is symmetric with respect to the center of the two sets of peaks, due to electron-hole symmetry.

Figure 2(b) shows the addition spectrum as a function of t for fixed C/C_g. For $t=0$, the spectrum shows the characteristic doublet structure of Fig. 1(b). An increasing t leads to a spreading of the doublets, due to the onset of miniband formation. At $t=0.24$ meV, the narrowing of the miniband gap stops and a pronounced anticrossing between the two minibands occurs, with a gap of U-t, similar to the anticrossing gap width in the linear 1D Hubbard model.[32] The miniband wings at the far side of the gap continue to spread out. This effect, however, has little experimental significance, for in reality, there are more than two energy levels in each dot. For larger t, the addition spectrum in the vicinity of the gap is only very weakly dependent upon t. In the limit of very

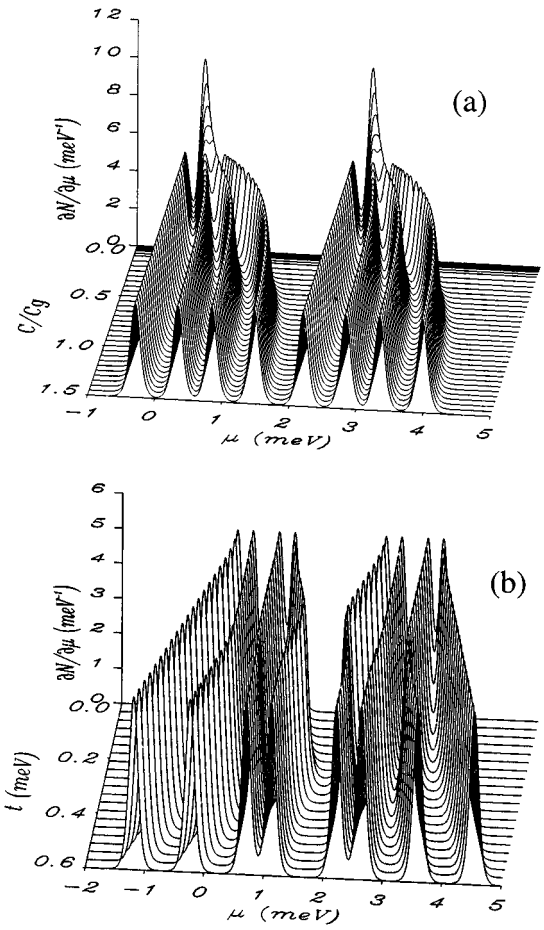

FIG. 2. (a) Evolution of the addition spectrum as C/C_g varies from 0 (back) to 1 (front). $t=0.15$ meV. (b) Addition spectrum as t varies from 0 (back) to 0.6 meV (front). $C/C_g=0.5$. In both plots $k_BT=50$ μeV, and $\Delta\varepsilon=0.5$ meV.

large t, the charge in the array is completely delocalized, and the addition of one electron to the array effectively adds 0.25 electrons to each dot. In contrast to Fig. 2(a), the spectrum shows an overall mirror symmetry with respect to the center of the gap between the two minibands, again due to electron-hole symmetry. Experimentally, the presence of an anticrossing would thus be a strong indication that t is tuned predominantly under a sweep of the back gate voltage.

Finally, we discuss the effects of disorder on the conductance and addition spectrum in the extended Hubbard model (Fig. 3). We have calculated the conductance of arrays where U_1, t_{12}, $\varepsilon_{1\alpha}$, or W_{12} is increased by 10%, while the other array parameters are kept constant. We find that the characteristic structure of the peak positions is maintained, and the peaks are only slightly shifted. The peak conductance, however, can be strongly influenced by disorder, particularly by disorder in U and $\varepsilon_{i\alpha}$ [Figs. 3(b) and 3(c)]. The peak amplitude can increase or decrease. Disorder in the energy levels of the dots tends to localize the charge, resulting in a strong modification of the wave-function overlap between the array and the leads. Furthermore, each type of disorder produces a typical modulation of the peak positions, which could be used to identify the dominant disorder in an experiment [Fig.

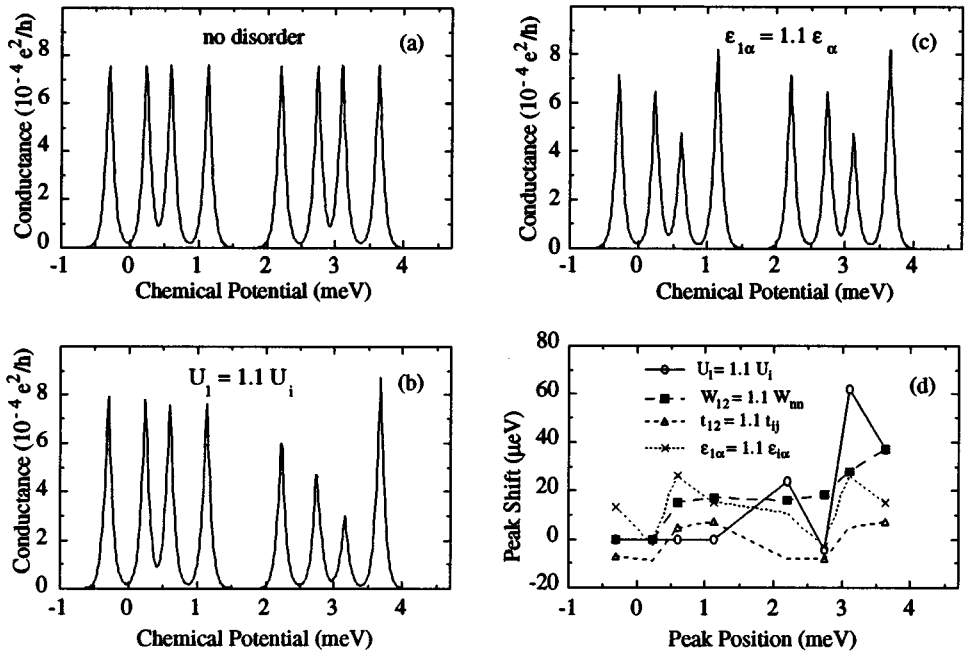

FIG. 3. Effect of disorder on the conductance. The peak positions are shifted only slightly, while the peak conductance can be strongly modified. (a) No disorder, $C/C_g = 0.5$, $t = 0.15$ meV, $\Delta\varepsilon = 0.5$ meV, and $k_B T = 50\ \mu$eV. (b) 10% disorder in U_i. (c) 10% disorder in $\varepsilon_{i\alpha}$. (d) Peak positions for each of the three cases.

3(d)]. However, the peak shifts generated by disorder in U_i and $\varepsilon_{i\alpha}$ differ qualitatively only in the lowest miniband. In our model the disorder in U has no effect at all, since there is not more than one electron in each cell.

In summary, we have calculated the addition spectrum and the conductance of a 2×2 quantum dot array in the extended Hubbard model. We find that, in contrast to array geometries studied experimentally so far, the addition spectrum of this array in the Hubbard model is distinctly different from that obtained in a classical charging model. We have developed an intuitive picture for these spectral structures in these limiting cases. To allow direct comparison with experiments, we have studied the general case, when both coherent tunneling between dots and interdot charging are present. Characteristic differences in the evolution of the spectra under a variation of C, compared to a variation of t, are found. An experimental study of this geometry should be able to clarify the origin of the observed peak splittings in small quantum-dot arrays. We have also shown that the array conductance is strongly affected by small amounts of disorder, in contrast to the more robust addition spectrum peak separations. Whether or not a general condition can be found for the Hubbard model and the charging model to produce qualitatively different addition spectra will be the subject of further work.[33]

It is a pleasure to thank S. das Sarma, C. L. Kane, and W. Zwerger for stimulating discussions. This work has been supported by the University of Pennsylvania, the Laboratory for Research on the Structure of Matter, and the Packard Foundation. A.T.J. acknowledges the support of the Alfred P. Sloan Foundation.

*Present address: ETH Zürich, am Hönggerberg, 8093 Zürich, Switzerland.

[1] C. A. Stafford and S. das Sarma, in *Quantum Transport in Ultrasmall Devices, Proceedings of the NATO Advanced Study Institute* (Plenum, New York, 1995), p. 445.
[2] Cheng Niu *et al.*, Phys. Rev. B **45**, 13 469 (1995).
[3] C. A. Stafford and S. das Sarma, Phys. Rev. Lett. **72**, 3590 (1994).
[4] C. S. Lent *et al.*, Appl. Phys. Lett. **62**, 714 (1993); P. D. Tougaw *et al.*, J. Appl. Phys. **74**, 3558 (1993); P. D. Tougaw and C. S. Lent, *ibid.* **75**, 1818 (1994); C. S. Lent and P. D. Tougaw, *ibid.* **75**, 4077 (1994).
[5] G. Klimeck *et al.*, Phys. Rev. B **50**, 2316 (1994).
[6] G. Chen *et al.*, Phys. Rev. B **50**, 8035 (1994).
[7] F. Ramirez *et al.*, Superlatt. Microstruct. **20**, 1 (1996).
[8] C. I. Duruöz *et al.*, Phys. Rev. Lett. **74**, 3237 (1995).
[9] M. Kemerink and L. W. Molenkamp, Appl. Phys. Lett. **65**, 1012 (1994).
[10] L. W. Molenkamp *et al.*, Phys. Rev. Lett. **75**, 4282 (1995).
[11] N. C. van der Vaart *et al.*, Phys. Rev. Lett. **74**, 4702 (1995).
[12] F. Hofmann *et al.*, Phys. Rev. B **51**, 13 872 (1995).
[13] F. R. Waugh *et al.*, Phys. Rev. Lett. **75**, 705 (1995); C. Livermore *et al.*, Science **274**, 1332 (1995).
[14] R. H. Blick *et al.*, Phys. Rev. B **53**, 7899 (1996).
[15] For a review, see A. N. Korotkov, in *Molecular Electronics*, edited by J. Jortner and M. A. Ratner (Blackwell, Oxford, 1996).
[16] C. B. Murray *et al.*, J. Am. Chem. Soc. **115**, 8706 (1993); A. P. Alivisatos, Science **271**, 933 (1996).
[17] C. Zhou *et al.*, Appl. Phys. Lett. **70**, 598 (1997).
[18] M. A. Kastner, Rev. Mod. Phys. **64**, 849 (1992).
[19] S. Tarucha *et al.*, Phys. Rev. Lett. **77**, 3613 (1996).
[20] D. V. Averin and K. K. Likharev, in *Mesoscopic Phenomena in Solids*, edited by B. L. Altshuler, P. A. Lee, and R. Webb (Elsevier, Amsterdam, 1991); A. A. Middleton and N. S. Wingreen, Phys. Rev. Lett. **71**, 3198 (1993).
[21] L. P. Kouwenhoven *et al.*, Phys. Rev. Lett. **65**, 361 (1990).

[22] R. J. Haug *et al.*, Surf. Sci. **263**, 415 (1992).
[23] Zhiming Yu *et al.* (unpublished).
[24] N. C. van der Vaart (private communication).
[25] We neglect the dot-to-lead capacitance and find for the configuration of Fig. 1(a): $U_i=(e^2/C_g)\times(C_g^2+4C_gC+2C^2)/[(C_g+2C)(C_g+4C)]$, $W_{\rm nn}=(e^2/C_g)\times C/(C_g+4C)$, and $W_{\rm diag}=(e^2/C_g)\times 2C^2/[(C_g+2C)(C_g+4C)]$.
[26] C. Lanzcos, J. Res. Natl. Bur. Stand. **45**, 255 (1950).
[27] E. Dagotto, Rev. Mod. Phys. **66**, 763 (1994).
[28] R. Ashoori *et al.*, Phys. Rev. Lett. **68**, 3088 (1992).
[29] H. Drexler *et al.*, Phys. Rev. Lett. **73**, 2252 (1994).
[30] C. W. J. Beenakker, Phys. Rev. B **44**, 1646 (1991).
[31] Y. Meir *et al.*, Phys. Rev. Lett. **66**, 1194 (1991).
[32] For a recent review, see E. B. Kolomeisky *et al.*, Rev. Mod. Phys. **68**, 175 (1996), and references therein.
[33] Z. Yu *et al.* (unpublished).